FEEDBACK CONTROL OF WALL TURBULENCE WITH WALL DEFORMATION

Takahide Endo
Nobuhide Kasagi
Yuji Suzuki

Department of Mechanical Engineering, The University of Tokyo
Hongo, Bunkyo-ku, Tokyo 113-8656, Japan

ABSTRACT

A simple control algorithm to determine wall deformation with wall variables is investigated based on physical arguments of turbulent coherent structure near the wall. It is found that the spanwise gradient of wall shear stresses are good indicators of strong quasi-streamwise vortex accompanied by the meandering of streak.

The performance of the proposed feedback control with wall variables and using arrayed deformable actuators is examined by using direct numerical simulation of turbulent channel flow. The mean friction drag is found to be reduced by 10%.

INTRODUCTION

From the view point of saving power and protecting the environment, it is strongly desired to develop efficient turbulence control techniques for drag reduction and heat transfer augmentation. Among various methodologies, active feedback control attracts much attention because of its large control effect with small control input (Moin & Bewley, 1994).

Choi *et al.* (1994) applied local blowing and suction on the wall of turbulent channel flow so that the wall-normal velocity induced by the quasi-streamwise vortex (QSV; hereafter) should be attenuated. They obtain 30% drag reduction in their direct numerical simulation (DNS). Bewley *et al.* (1993) employed sub-optimal control theory (Choi *et al.*, 1993) in order to optimize wall blowing/suction distribution and obtain similar results. Although their algorithm needs the flow variables inside the flow domain to be known, Lee *et al.* (1997, 1998) have recently developed control algorithms, in which only the variables on a wall surface are required based on neural networks and sub-optimal control theory.

In the present study, an alternative control algorithm using only wall variables is investigated based on physical arguments. Since coherent structures, especially QSV play a dominant role in near-wall turbulent transport mechanisms (Robinson, 1991; Kasagi *et al.*, 1995), an efficient control is expected to be established through selective manipulation of those structures.

Sensors and actuators for turbulence active control should have the same length and time scales as those of the near-wall coherent structures. Recently, prototypes of distributed micro devices have been fabricated with the aid of microelectromechanical systems (MEMS) technology (Ho & Tai, 1998).

Among many types of actuators, wall deformation is considered to be one of the most promising candidate, because of its robustness against the hostile environment. Carlson & Lumley (1996) employed a Gaussian-shaped bump elongated in the spanwise direction with its maximum height of 12 viscous length in a minimal channel flow. They found that when the bump is raised underneath high-speed region, it lifts the faster moving fluid away from the wall, and thus the friction drag is decreased as much as 7%. However, the effect of wall motion on the near-wall coherent structures and hence the friction drag mechanism remains to be resolved.

The objectives of the present study are to evaluate arrayed wall deformation actuators for drag reduction and to develop a control algorithm using only wall variables based on the dynamics of near-wall coherent structure. For this purpose, we employ DNS of turbulent channel flow with deformable walls.

NUMERICAL PROCEDURE

The flow geometry and the coordinate system are shown in Fig. 1. The governing equations are the in-

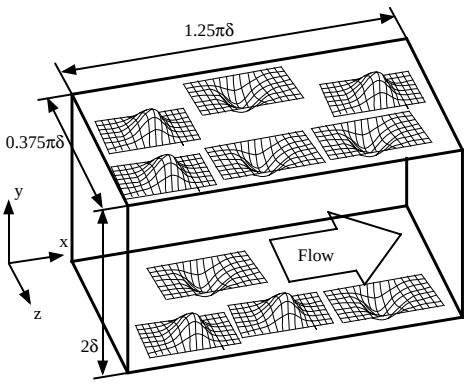

Figure 1. Flow geometry and coordinate system.

compressive Navier-Stokes equations and the continuity equation. The wall deformation is described with a boundary-fitted coordinate system for moving boundary. Periodic boundary conditions are employed in the streamwise ($x-$) and spanwise ($z-$) directions, while non-slip boundary condition is imposed on the top and bottom deformable walls.

A modified Crank-Nicolson type fractional-step method (Choi & Moin, 1994) is used for the time advancement, while a second-order finite difference scheme is employed for the spatial discretization of both flow variables and metrics on a staggered mesh (Mito & Kasagi, 1998). The pressure Poisson equation is solved with the multi-grid method (Demuren & Ibraheem, 1998). Successive over relaxation (SOR) method is adopted in the finest and middle meshes, whilst an incomplete LU conjugate gradient squared (ILUCGS) method in the coarsest mesh.

The size of the computational volume is $1.25\pi\delta$ in the streamwise direction and $0.375\pi\delta$ in the spanwise direction (where, δ is the channel half width), which correspond to about 590 and 180 viscous length scale, respectively. It is about 2.5 and 1.5 times larger than the so-called minimal flow unit (Jiménez & Moin, 1991). Hereafter, all the parameters with a superscript + represent quantities non-dimensionalized by the friction velocity u_τ in the unactuated channel flow and the kinematic viscosity ν.

The number of grid points is 48, 97 and 48 in the $x-, y-$ and $z-$directions, respectively. Uniform meshes are used in the $x-$ and $z-$directions with spacings $\triangle x^+ = 12$ and $\triangle z^+ = 3.7$. A non-uniform mesh with a hyperbolic tangent distribution is used in the $y-$ direction. The first mesh point away from the wall is given at $y^+ = 0.25$.

The computational time step is $0.33\nu/u_\tau^2$. The simulation is performed under the constant flow rate condition throughout the present study. The Reynolds number based on the bulk mean velocity U_b and the channel width 2δ is 4600 (about 150 based on u_τ and δ for the unactuated turbulent channel flow). An instantaneous flow field of a fully-developed turbulent channel flow was used for the initial condition.

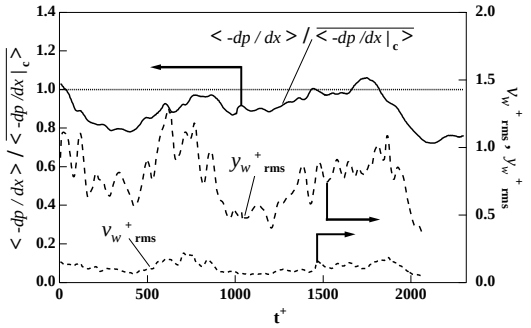

Figure 2. Time traces of mean pressure gradient and the rms values of y_w and v_w.

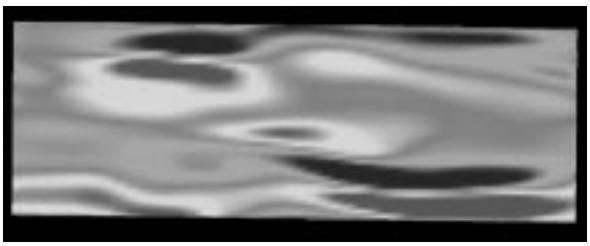

Figure 3. Instantaneous wall deformation ($t^+ = 630$). Flow : left to right, Black to Gray : $y_w^+ = -2$ to 2.

ACTIVE CANCELLATION BY WALL DEFORMATION

In the first stage of the present study, a simple feedback algorithm is employed, in order to evaluate the effect of wall deformation in drag reduction and estimate the typical spatio-temporal scale of the deformation. In the same manner as the active cancellation control (Choi *et al.*, 1994), the wall velocity, v_w, is determined as follows:

$$v_w^+(t_{n+1}) = -\left(v_s^+(t_n) - << v_s^+(t_n) >>\right) - 0.31 y_w^+(t_n), \quad (1)$$

where t_n denotes the time step, v_s is the wall-normal velocity at $y/\delta = 0.1\,(y^+ \sim 15)$, while y_w is the displacement of the wall. The double bracket $<< \chi >>$ denotes an ensemble average of quantity χ in the $x-z$ plane at each time step, and superscript n is the time step. The second term of the right hand side of Eq. (1) is a damping term to suppress excessive wall deformation.

Time trace of the volume-averaged streamwise pressure gradient, which is normalized by that in the unactuated case is shown in Fig. 2. The friction drag is decreased to as large as 28% at $t^+ = 2190$ with a long-term fluctuation, and the mean drag reduction rate during $t^+ = 0 \sim 5000$ is about 10%. As also shown in Fig. 2, the rms values of the wall displacement and the wall velocity are $1.0\nu/u_\tau$ and $0.15u_\tau$, respectively. Wall roughness with its size less than $y^+ = 5$ is categorized as hydraulically smooth (Schlichting, 1960), and may not affect much to the turbulence coherent structure. On the other hand, the rms value of the wall

Table 1. Four events at the edge of meandering streaks.

Event	$\partial u'/\partial x$	$\partial u'/\partial z$
E1	Positive	Positive
E2	Negative	Positive
E3	Negative	Negative
E4	Positive	Negative

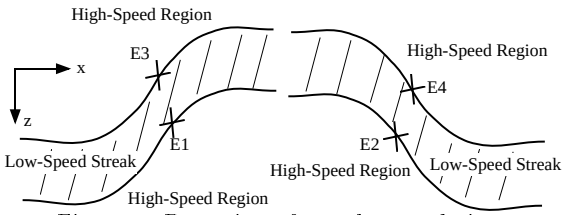

Figure 4. Detection of streak meandering.

velocity is in the same order of that of the wall-normal velocity fluctuation at $y^+ = 10$. According to Choi *et al.* (1994), when the blowing/suction from the wall is employed exactly opposite to the wall-normal velocity at $y^+ = 10$, the friction drag reduced significantly. Therefore, the drag reduction presently obtained is due to the wall-normal velocity of the wall rather than the displacement of the wall. Note that the displacement and the velocity of the wall deformation in the present study are much smaller than those of Carlson & Lumley (1996), which are $12.0\nu/u_\tau$ and $1.0u_\tau$, respectively.

Figure 3 shows instantaneous wall deformation. It is evident that the deformation is much elongated in the streamwise direction. The typical scales estimated from the two-dimensional $(x-z)$ spectrum of the wall velocity v_w are $(m^+_{vx}, m^+_{vz}) = (300, 45)$, the latter of which is about half the mean spanwise spacing of the near-wall streaks (not shown here).

DETECTION OF QUASI-STREAMWISE VORTEX BY SENSING WALL VARIABLES

It is now evident that wall deformation determined by the active cancellation control scheme is effective in drag reduction, once the wall-normal velocity inside the flow domain is given. However, it is impractical to measure flow variables at many points away from the wall, especially right above the deforming wall actuators. In this section, a new algorithm to determine the wall velocity based on the information obtained by wall sensors is proposed from the argument on the dynamics of near-wall coherent structures.

It is well known that the near-wall streaky structure does not always flow straight in the streamwise direction, but often meanders in the spanwise direction. Johansson *et al.* (1991) showed by using a conditional average that the turbulent production was very large near the streaky structures asymmetric in the spanwise direction. Hamilton *et al.* (1995) pointed out that the QSV and the streaky structure had close dynamical relationship, and the meandering plays an important role in a temporally quasi-cyclic process of regeneration. Jeong *et al.* (1997) proposed a schematic model of the QSV alternatively tilting in the $x-z$ plane with the meandering of the near-wall low-speed streak.

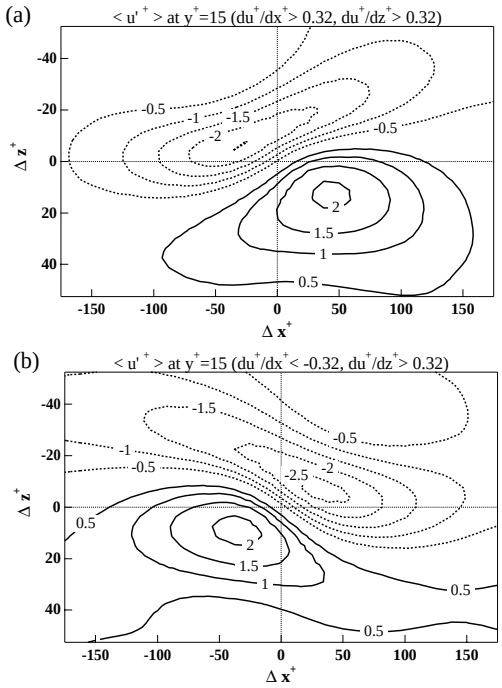

Figure 5. Conditional-averaged streamwise velocity contours at $y^+ = 15$. (a) event E1, (b) event E2.

Figure 4 shows a schematic diagram of streaks meandering in the spanwise direction. Depending on the signs of velocity gradients $\partial u'/\partial x$ and $\partial u'/\partial z$, the edges of meandering streaks can be grouped into four events as tabulated in Table. 1. Note that E1 and E4, and, E2 and E3 are respectively mirror symmetry in the spanwise direction.

In order to examine flow characteristics for each event, conditional averages of fully-developed plane channel flow are calculated, given the condition of the sign of $\partial u^+/\partial x^+$ and $\partial u^+/\partial z^+$ at $y^+ = 15$. A threshold of 0.32 is used for both gradients to capture strong meandering phenomena.

Figure 5 shows contours of conditional-averaged streamwise velocity $< u'^+ >$ at $y^+ = 15$ for events E1 and E2. Contours of negative $< u'^+ >$ corresponding to the low-speed streak are elongated in the streamwise direction, and tilted in the spanwise direction in both events. The detection point (at $\Delta x^+ = \Delta z^+ = 0$) corresponds to the upstream and downstream edges of the streak in E1 and E2, respectively, as depicted in Fig. 4.

Figure 6 shows contours of conditional-averaged streamwise vorticity $< \omega_x^+ >$ at $y^+ = 15$ for events E1 and E2. In event E1, a large peak in ω_x^+ exists at the detection point. Thus, QSV should often appear with event E1. On the other hand, the magnitude of ω_x is very small in event E2. The present result is in accordance with the conceptual model proposed by Jo-

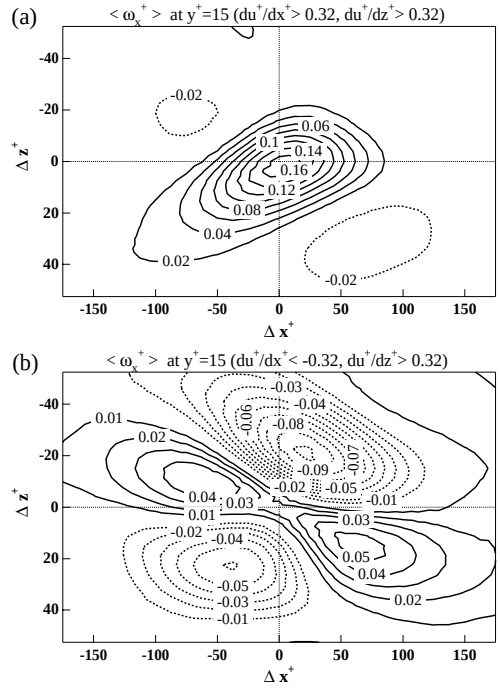

Figure 6. Conditional-averaged streamwise vorticity contours at $y^+ = 15$. (a) event E1, (b) event E2.

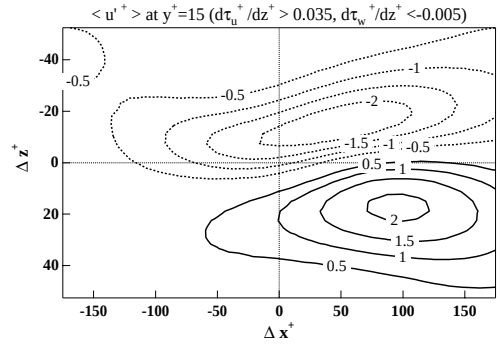

Figure 7. Contours of streamwise velocity at $y^+ = 15$, given the conditions $\partial\tau_u^+/\partial z^+ > 0.035$ and $\partial\tau_w^+/\partial z^+ < -0.005$.

eng *et al.* (1997) showing that QSV is located on the upstream side of meandering low-speed streak.

The equation of streamwise vorticity ω_x^+ can be written as follows :

$$\frac{D\omega_x^+}{Dt^+} = \omega_x^+ \frac{\partial u^+}{\partial x^+} - \frac{\partial w^+}{\partial x^+}\frac{\partial u^+}{\partial y^+} + \frac{\partial v^+}{\partial x^+}\frac{\partial u^+}{\partial z^+} + \nabla^2\omega_x^+, \quad (2)$$

where the first term of the right hand side of Eq. (2) is the stretching term, while the second and the third correspond to tilting and twisting terms, respectively. Since $(\partial w/\partial x)\cdot(\partial u/\partial y)$ is the largest term in Eq. (2), ω_x is produced by the tilting of ω_y in its early stage (Brooke & Hanratty, 1993). Once ω_x is formed, however, the stretching terms may be dominant, since ω_x has a finite absolute value (Sendstad & Moin, 1992). Therefore, the peak in ω_x accompanied with event

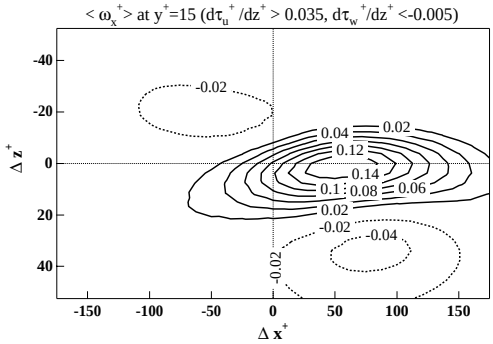

Figure 8. Contours of streamwise vorticity at $y^+ = 15$, given the conditions $\partial\tau_u^+/\partial z^+ > 0.035$ and $\partial\tau_w^+/\partial z^+ < -0.005$.

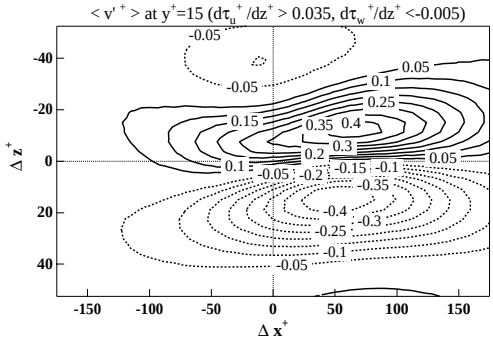

Figure 9. Contours of wall-normal velocity at $y^+ = 15$, given the conditions $\partial\tau_u^+/\partial z^+ > 0.035$ and $\partial\tau_w^+/\partial z^+ < -0.005$.

E1 corresponds to the large production of ω_x by the stretching term $\omega_x \cdot (\partial u/\partial x)$, since $\partial u/\partial x$ is positive. For event E2, $\partial u/\partial x$ is negative, so that the magnitude of ω_x should be decreased. Thus, the streak meandering substantially contributes to the evolution of ω_x and the regeneration mechanism of the QSV.

It is now clear that the meandering of streaks has an important role in the dynamics of coherent structure, and it might be possible to detect strong QSV by measuring the flow parameters on the wall. Although it is not shown here, we tested several candidate parameters for events E1 $\sim$ E4, and found that the wall shear stress fluctuations τ_u^+ ($\equiv \partial u'^+/\partial y^+|_w$) and τ_w^+ ($\equiv \partial w'^+/\partial y^+|_w$) are good indicators. The condition is chosen as $\partial\tau_u^+/\partial z^+ > 0.035$ and $\partial\tau_w^+/\partial z^+ < -0.005$.

The contours of conditional-averaged streamwise velocity fluctuation at $y^+ = 15$ are shown in Fig. 7. Although the tilting angle of the streak is slightly smaller than that obtained with the condition at $y^+ = 15$ in Fig. 5, streak meandering corresponding to event E1 is well captured at a location of $\triangle x^+ \doteqdot 50$ downstream from the detection point. There is also captured a large positive peak of ω_x^+ at $y^+ = 15$ in the region where the streak meanders as shown in Fig. 8.

Figure 9 shows the conditional-averaged wall-normal velocity $< v'^+ >$ at $y^+ = 15$, given the some wall shear

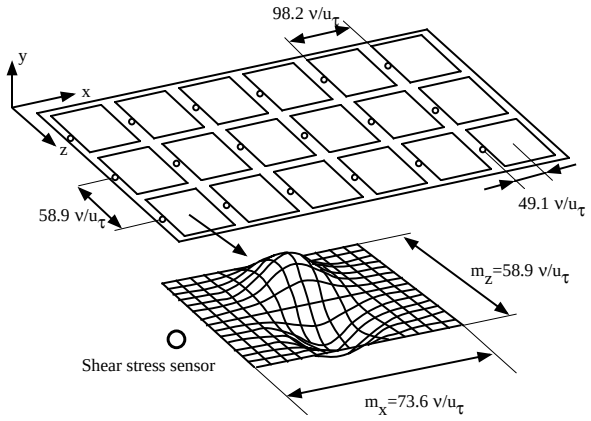

Figure 10. Arrangement of deformable actuators.

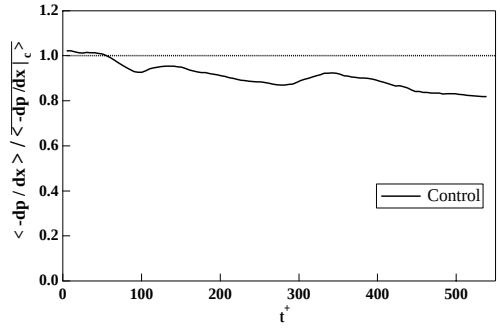

Figure 11. Time trace of mean pressure gradient.

stress conditions. Positive and negative peaks aligned in the spanwise direction, which respectively correspond to the ejection and sweep motions, are observed. The spanwise distance of the positive and negative peaks is about $30\nu/u_\tau$, which is the same dimension with the mean diameter of QSV (Robinson, 1991). Therefore, the wall deformation for the active cancellation should be determined by using $\partial\tau_u/\partial z$ and $\partial\tau_w/\partial z$ in such a way that the wall velocity would be opposite to the wall-normal velocity at $y^+ = 15$ shown in Fig. 9.

Lee *et al.* (1997, 1998) showed that wall blowing/ suction roughly proportional to $\partial\tau_w/\partial z$ can reduce drag significantly. The present control scheme based on the dynamics of the near-wall coherent structures is similar to their algorithm in this sense. However, the location for actuation is about $50\nu/u_\tau$ downstream of the sensing location, and this fact would be advantageous in real applications since actuators can be separated from sensors.

FEEDBACK CONTROL WITH ARRAYED DEFORMABLE ACTUATORS

Figure 10 shows a proposed arrangement of shear stress sensors and deformable actuators. Since the conditional-averaged wall-normal velocity distribution for event E1 exhibits a pair of positive and negative peaks aligned in the spanwise direction as shown in Fig. 9, each actuator is assumed to deform in a si-

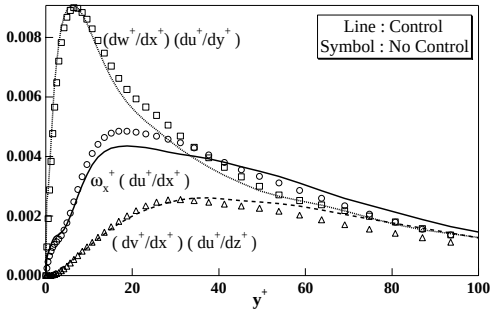

Figure 12. Production term in the streamwise vorticity equation.

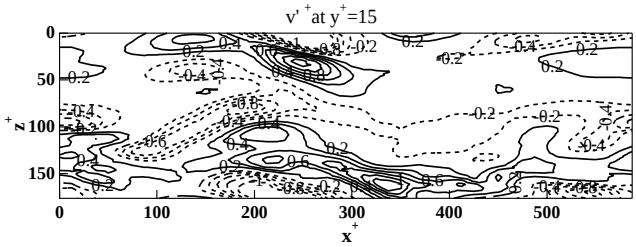

Figure 13. Instantaneous wall-normal velocity at $y^+ = 15$.

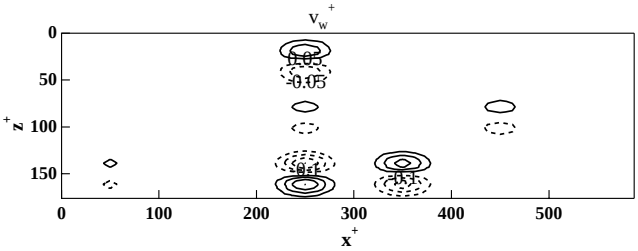

Figure 14. Instantaneous wall velocity.

nusoidal shape in the spanwise direction. The spanwise dimension of the actuator is chosen as $m_z^+ = 58.9$, so that the distance between the peak and trough is about $30\nu/u_\tau$. A shear stress sensor is assumed to be located at $50\nu/u_\tau$ upstream from the center of each actuator. In the present study, 6×3 (streamwise $\times$ spanwise) actuators are arranged with a regular pitch on both walls of the channel.

Each sensor measures spanwise gradients of shear stresses, $\partial\tau_u/\partial z$ and $\partial\tau_w/\partial z$. When $\partial\tau_w/\partial z$ is negative, the maximum wall velocity at the peak/ trough of the actuator v_m is determined by:

$$v_m^+(t_{n+1}) = \alpha \tanh\left(\frac{\partial\tau_u^+(t_n)}{\partial z^+}/\beta\right) - \gamma y_m^+(t_n), \qquad (3)$$

where y_m is the wall displacement at the peak/ trough, and α, β, and γ are control parameters, respectively. The wall velocity of each grid point on the actuator is given by

$$v_w^+(t_{n+1}) = v_m^+(t_{n+1}) \times \exp\left[-\frac{(x^+ - x_c^+)^2}{\sigma_x^2} - \frac{(z^+ - z_c^+)^2}{\sigma_z^2}\right]$$

$$\times \sin\left[\frac{2\pi(z^+ - z_c^+)}{m_z^+}\right], \qquad (4)$$

where x_c and z_c denote the location of the center of the actuator. The parameters are determined through preliminary computations, and chosen as $\alpha = 1.39, \beta = 0.05, \gamma = 0.31, \sigma_x = 0.165 m_x^+$, and $\sigma_z = 0.185 m_z^+$, respectively.

Figure 11 shows a time trace of the volume-averaged streamwise pressure gradient. A maximum drag reduction rate of 18% is obtained at $t^+ = 530$. The mean drag reduction rate during $t^+ = 0 \sim 530$ is about 10%. Therefore, the present control scheme with arrayed actuators should provide almost the same control results as the simple feedback law with arbitrary wall deformation shown in Fig. 2.

Although it is not shown here, all components of the Reynolds stresses are decreased near the wall, and the viscous sublayer is thickened, which is often observed in drag reducing wall turbulence.

Figure 12 shows the production terms in Eq. (2). The stretching term $\omega_x^+ \cdot (\partial u^+/\partial x^+)$ is selectively decreased near the wall. This is because the wall deformation with the present control algorithm is large near the meandering of streaks, where the stretching term is dominant.

Figures 13 and 14 show instantaneous contours of v'^+ at $y^+ = 15$ and v_w^+, respectively. It is found from these figures that the present control method can provide wall velocity opposite to most strong vortices, although, the correlation between v'^+ at $y^+ = 15$ and v_w^+ is about -0.4. Therefore, further optimization of control parameters would be possible to obtain larger drag reduction.

CONCLUSIONS

DNS of turbulent channel flow was made to evaluate feedback control with arrayed deformable actuators. A new realizable control method based on physical arguments of the turbulent coherent structures is proposed. The quasi-streamwise vortex accompanied with streak meandering is detected by sensing shear stress gradients at the wall. A pair of strong wall-normal velocity components aligned in the spanwise direction at about 50 viscous length downstream from the sensing location are successfully captured by employing the combined conditions of $\partial\tau_u/\partial z$ and $\partial\tau_w/\partial z$ on the wall. The mean friction drag is reduced by 10% with the arrayed actuators, of which deformation impede the wall-normal velocities captured.

References

Bewley, T.R., Choi, H., Temam R., and Moin P., 1993, "Optimal feedback control of turbulent channel flow," CTR Annual Research Briefs, Stanford Univ., pp. 3-14.

Brooke, J.W., and Hanratty, T.J., 1993, "Origin of turbulence-producing eddies in a channel flow," Phys. Fluids A, Vol. 5, pp. 1011-1022.

Carlson, H.A., & Lumly, J.L., 1996, "Active control in the turbulent wall layer of a minimal flow unit," J. Fluid Mech., Vol. 329, pp. 341-371.

Choi, H., Temam, R., Moin, P., & Kim, J., 1993, "Feedback control for unsteady flow and its application to the stochastic Burgers equation," J. Fluid Mech., Vol. 253, pp. 509-543.

Choi, H., Moin, P., and Kim, J., 1994, "Active turbulence control for drag reduction in wall-bounded flows," J. Fluid Mech., Vol. 262, pp. 75-110.

Choi, H., and Moin, P., 1994, "Effects of the computational time step on numerical solutions of turbulent flow," J. Comput. Phys. Vol 113, pp. 1-4.

Demuren, A.O., and Ibraheem, S.O., 1998, "Multigrid method for the Euler and Navier-Stokes equations," AIAA J., Vol. 36, pp. 31-37.

Hamilton, J. M., Kim, J., and Waleffe, F., 1995, "Regeneration mechanism of near-wall turbulence structures," J. Fluid Mech., Vol. 287, pp. 317-348.

Ho, C-M., and Tai, Y-C., 1998, "Micro-Electro-Mechanical-Systems (MEMS) and fluid flows," Annu. Rev. Fluid Mech, Vol. 30, pp. 579-612.

Jiménez, J., and Moin, P., 1991, "The minimal flow unit in near-wall turbulence," J. Fluid Mech., Vol. 225, pp. 213-240.

Joeng, J., Hussain, F., Schoppa, W., and Kim, J., 1997, "Coherent structures near the wall in a turbulent channel flow," J. Fluid Mech., Vol. 332, pp. 185-214.

Johanson, A.V., Alfredsson, P.H., and Kim, J., 1991, "Evolution and dynamics of shear-layer structures in near-wall turbulence," J. Fluid Mech., Vol. 224, pp. 579-599.

Kasagi, N., Sumitani, Y., Suzuki, Y., and Iida, O., 1995, "Kinematics of the quasi-coherent vortical structure in near-wall turbulence," Int. J. Heat & Fluid Flow, Vol. 16, pp. 2-10.

Lee, C., Kim, J., Babcock, B., and Goodman, R., 1997, "Application of neural networks to turbulence control for drag reduction," Phys. Fluids, Vol. 9, pp. 1740-1747.

Lee, C., Kim, J., and Choi, H., 1998, "Suboptimal control of turbulent channel flow for drag reduction," J. Fluid Mech., Vol. 358, pp. 245-258.

Mito, Y., and Kasagi, N., 1998, "DNS study of turbulence modification with streamwise-uniform sinusoidal wall-oscillation," Int. J. Heat & Fluid Flow, Vol 19, pp. 470-481.

Moin, P., and Bewley, T., 1994, "Feedback control of turbulence," Appl. Mech. Rev., Vol. 47, S3-S13.

Robinson, S.K., 1991, "Coherent motions in the turbulent boundary layer," Annu. Rev. Fluid Mech., Vol. 23, pp. 601-639.

Schlichting, H., 1960, "Boundary Layer Theory," McGraw-Hill, New York.

Sendstad, O., and Moin, P., 1992, "The near wall mechanics of three-dimensional turbulent boundary layers," Rep. TF-57, Dept. Mech. Eng., Stanford Univ.